duced to ~10% when compared with that of the untreated control (8 versus 81 PSL units). The apparent half-life of core protein was calculated to be 3 hours, whereas its half-life in the untreated sample exceeded 24 hours (Fig. 4A). When Bay 39-5493 was added to the cells at the beginning of the chase, no depletion of core protein was observed compared with untreated controls (supporting online text S9, fig. S6). This result was to be expected, assuming that within 10 min of labeling, most newly synthesized core protein was aggregated (supporting online text S3) and thereby rescued from the activity of the drug. Apparently, it was only when particle formation was inhibited by HAP that core protein did not become stabilized and was instead degraded. This process was proteasome mediated (Fig. 4B): The addition of the proteasome inhibitor lactacystin induced accumulation of HBV core protein at 4 hours (84 versus 34 PSL units) and even at 8 h of chase (58 versus 25 PSL units), whereas all of the core protein had virtually disappeared at this time point in the Bay 41-4109–treated samples that were devoid of lactacystin. In conclusion, our data provide strong evidence for an inhibition of particle formation as the primary event and an increased degradation of core protein as a consequence of this mode of HAP action.

We present a substance class for the treatment of HBV infection that displays a highly specific antiviral principle, namely, inhibition of capsid formation, concomitant with a reduced half-life of the core protein. The candidate, Bay 41-4109, may become a valuable addition to future therapy (mono- or combination-therapy regimens) in light of its specific mechanism of action. It has a demonstrated efficacy in HBV transgenic mice (*4*) and a suitable preclinical pharmacokinetic and toxicology profile (supporting online text S10). The clinical efficacy of this treatment modality of HBV infection will now need to be demonstrated.

References and Notes

1. K. Deres, H. Rübsamen-Waigmann, *Infection* **27** (Suppl. 2), S45 (1999).
2. K. P. Fischer, K. S. Gutfreund, D. L. Tyrrell, *Drug Resist. Updates* **4**, 118 (2001).
3. W. E. Delaney IV, S. Locarnini, T. Shaw, *Antivir. Chem. Chemother.* **12**, 1 (2001).
4. O. Weber *et al.*, *Antiviral Res.* **54**, 69 (2002).
5. R. W. King *et al.*, *Antimicrob. Agents Chemother.* **42**, 3179 (1998).
6. M. Nassal, *Curr. Top. Microbiol. Immunol.* **214**, 297 (1996).
7. M. A. Sells, M. L. Chen, G. Acs, *Proc. Natl. Acad. Sci. U.S.A.* **84**, 1005 (1987).
8. M. Nassal, *J. Virol.* **66**, 4107 (1992).
9. C. Lamberts, M. Nassal, I. Velhagen, H. Zentgraf, C. H. Schröder, *J. Virol.* **67**, 3756 (1993).
10. M. L. Doyle, *Curr. Opin. Biotechnol.* **8**, 31 (1997).
11. Materials and methods are available as supporting material on *Science* Online.

12. We thank M. Kraft, S. Kellermann, H. Küper, I. Leckebusch, K. Riedel, and M. Korkowski for technical support and D. Cramer for the artwork. We also thank H.-J. Schlicht (University of Ulm, Germany) for providing rabbit anti-HBV core polyclonal antisera and DHBV core protein and M. Nassal (University of Freiburg, Germany) for providing the plasmids pCH-9/3091, pCS1a-C1, and pPLc-EHII. We thank G. Hewlett for critically reading the manuscript. This publication is dedicated to the late Ulrich Niewöhner. We miss his scientific excellence, inspiring mind, and warm personality.

Supporting Online Material
www.sciencemag.org/cgi/content/full/299/5608/893/DC1
Materials and Methods
SOM Text S1 to S10
Figs. S1 to S6
References

12 August 2002; accepted 6 January 2003

Mitochondrial Biogenesis in Mammals: The Role of Endogenous Nitric Oxide

Enzo Nisoli,[1,2]*† Emilio Clementi,[3,4]* Clara Paolucci,[3] Valeria Cozzi,[1] Cristina Tonello,[1] Clara Sciorati,[3] Renata Bracale,[1] Alessandra Valerio,[5] Maura Francolini,[6] Salvador Moncada,[7] Michele O. Carruba[1,2]

Nitric oxide was found to trigger mitochondrial biogenesis in cells as diverse as brown adipocytes and 3T3-L1, U937, and HeLa cells. This effect of nitric oxide was dependent on guanosine 3′,5′-monophosphate (cGMP) and was mediated by the induction of peroxisome proliferator–activated receptor γ coactivator 1α, a master regulator of mitochondrial biogenesis. Moreover, the mitochondrial biogenesis induced by exposure to cold was markedly reduced in brown adipose tissue of endothelial nitric oxide synthase null-mutant (eNOS$^{-/-}$) mice, which had a reduced metabolic rate and accelerated weight gain as compared to wild-type mice. Thus, a nitric oxide–cGMP–dependent pathway controls mitochondrial biogenesis and body energy balance.

Mitochondria in mature brown adipocytes are more numerous and larger than those of other cell types. Furthermore, their inner mitochondrial membrane contains uncoupling protein 1 (UCP1), which diverts energy from adenosine triphosphate synthesis to thermogenesis (*1*). NO modulates biological functions in these cells, including inhibition of proliferation (*2*, *3*), but its role in the genesis of their mitochondria has not been studied.

Primary cultures of mouse brown adipocyte precursors (*4*) were treated with or without the NO donor *S*-nitrosoacetyl penicillamine (SNAP), and mitochondrial biogenesis was investigated (*5*). Mitochondrial DNA (mtDNA) content in untreated brown adipocytes increased progressively (by 300 ± 15% and 600 ± 20% at days 4 and 6 of culture, respectively; $n = 6$ experiments), which is consistent with the adipocyte rate of spontaneous differentiation in culture (*2*). Increasing concentrations of SNAP (10 to 300 μM) further increased mtDNA content (by 220 ± 12% and 240 ± 11% with 100 μM SNAP over values observed in untreated controls at days 4 and 6, respectively; $P < 0.01$, $n = 6$ experiments) (Fig. 1A and fig. S1). Supplementation of the medium with 50 μM oxyhemoglobin, which scavenges NO, completely abolished this action of SNAP (Fig. 1A), suggesting that the effect was indeed due to generation of NO. Treatment with 100 μM SNAP for 4 days caused a parallel increase over untreated controls of the other parameters investigated: MitoTracker fluorescence signal (Fig. 1B and fig. S1); expression of cytochrome c oxidase subunit IV (COX IV) and cytochrome c (Cyt c) (increased by 210 ± 18% and 480 ± 29%, respectively, $P < 0.01$, as assessed by immunoblotting on whole cell lysates, $n = 5$ experiments) (Fig. 1C); and number of mitochondria per cell (increased by 45 ± 3%, $n = 5$ experiments) (Fig. 1D). Mitochondria of SNAP-treated brown adipocytes were large and heterogeneous in size. Quantitative morphometry indicated a 61% increase in mean mitochondrial volume density (total mitochondrial area divided by total cytoplasmic area, 2.37 ± 0.15 versus 1.47 ± 0.11 μm^3 per μm^3 of cell cyto-

[1]Department of Preclinical Sciences, Center for Study and Research on Obesity, Luigi Sacco Hospital, University of Milan, Milan 20157, Italy. [2]Istituto Auxologico Italiano, Milan 20149, Italy. [3]DIBIT-H San Raffaele Institute, Milan 20132, Italy. [4]Department of Pharmaco-Biology, University of Calabria, Rende 87036, Italy. [5]Department of Biomedical Sciences and Biotechnology, University of Brescia, Brescia 25123, Italy. [6]Consiglio Nazionale delle Ricerche Institute of Neuroscience, Cellular and Molecular Pharmacology Section, Milan 20129, Italy. [7]The Wolfson Institute for Biomedical Research, University College London, London WC1E 6BT, UK.

*These authors contributed equally to this work.
†To whom correspondence should be addressed. E-mail: enzo.nisoli@unimi.it

Downloaded from www.sciencemag.org on March 2, 2007

plasm, $P < 0.01$, $n = 50$ cells). Similar results were obtained with *S*-nitroso-L-glutathione, further indicating that NO can trigger mitochondrial biogenesis in brown adipocytes.

Peroxisome proliferator–activated receptor γ (PPARγ) coactivator 1α (PGC-1α) is a master regulator of mitochondrial biogenesis in brown adipose tissue (BAT) and in cardiac and skeletal muscle (*6*–*8*). PGC-1α stimulates expression of nuclear respiratory factor 1 (NRF-1) and mitochondrial transcription factor A (mtTFA), initiating the expression of nuclear and mitochondrial genes that encode mitochondrial proteins (*6*, *7*, *9*). Cold exposure and exercise trigger the expression of PGC-1α through activation of β_3-adrenergic receptors and increases in intracellular cyclic adenosine monophosphate and Ca^{2+} (*7*, *10*, *11*). These signals stimulate NO production in brown adipocytes (*2*), indicating that different stimuli may control mitochondrial number and thus brown fat function via a common pathway. We investigated whether NO-induced mitochondrial biogenesis occurred through activation of PGC-1α. Treatment with 100 μM SNAP for 4 days triggered expression of PGC-1α, NRF-1, and mtTFA, albeit to different degrees (Fig. 1E). PGC-1β, a homolog of PGC-1α (*12*), was not induced by SNAP. The relevance of PGC-1α was further assessed using a morpholino PGC-1α antisense oligomer (fig. S2). Neither the PGC-1α antisense oligomer nor its control oligomers modified the mtDNA content or MitoTracker fluorescence in resting, untreated cells. However, in the presence of the PGC-1α antisense oligomer, the SNAP-induced increase in mtDNA content was significantly reduced (by 32 ± 3% versus cells treated with SNAP alone; $P < 0.05$, $n = 5$ experiments), as was the increase in MitoTracker fluorescence (Fig. 1, B and E, insets). Thus, NO-induced mitochondrial biogenesis required induction of PGC-1α expression.

In order to investigate whether NO-mediated mitochondrial biogenesis is dependent on guanosine 3′,5′-monophosphate (cyclic GMP, or cGMP), we examined the effects of the membrane-permeable cGMP analog 8 Br-cGMP and of the selective guanylate cyclase inhibitor 1H-[1,2,4]oxadiazolo[4,3-a] quinoxalin-1-one (ODQ). Treatment for 4 days with 1 mM 8 Br-cGMP mimicked the effects of NO, i.e., increases in mtDNA content, MitoTracker fluorescence signal, and COX IV and Cyt c protein expression, as well as in PGC-1α, NRF-1, and mtTFA mRNA levels (Fig. 1). Consistently, co-incubation with ODQ (1 μM) reversed the mitochondrial biogenesis induced by SNAP, whereas ODQ alone had no effect (Fig. 1). Thus, mitochondrial biogenesis in brown adipocytes was triggered by NO through activation of cGMP-dependent signal transduc-

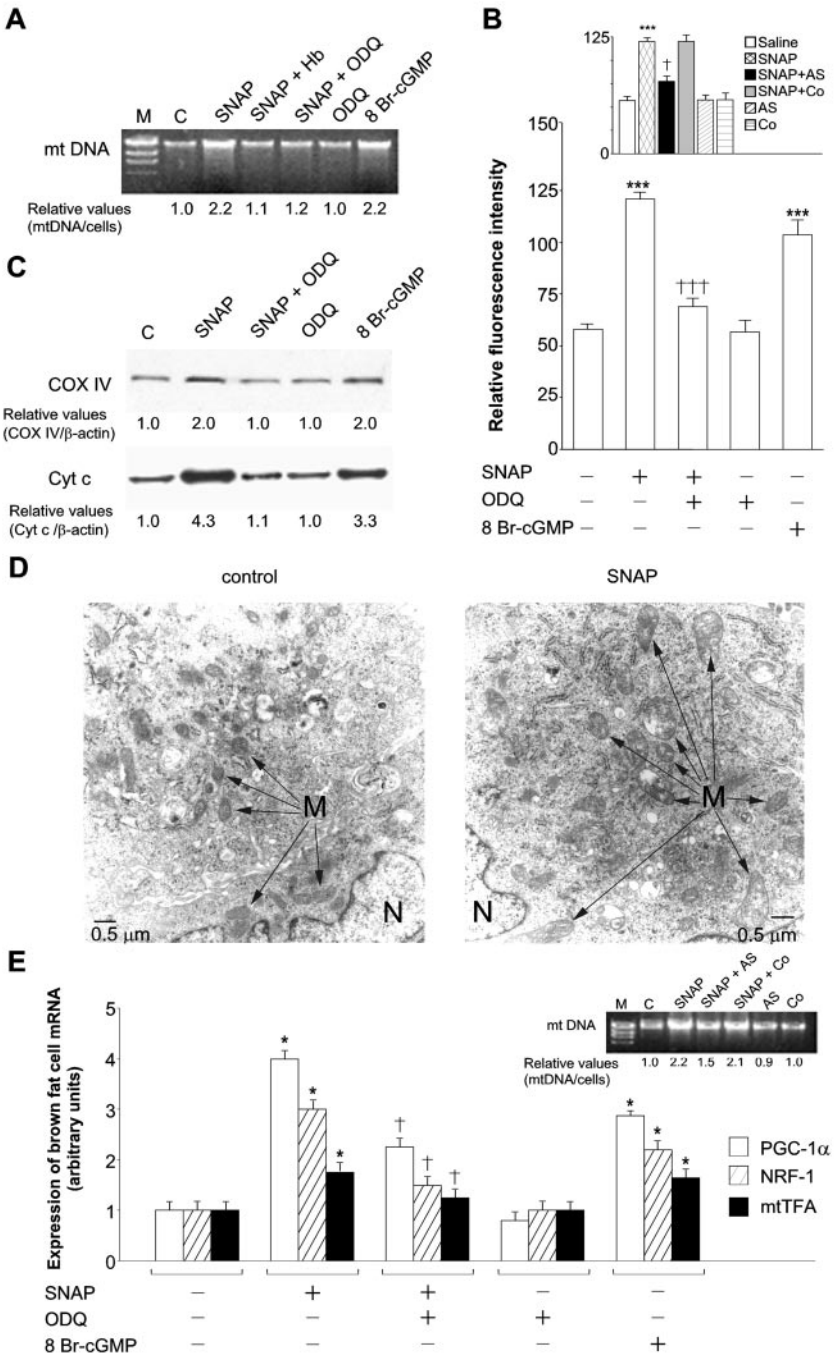

Fig. 1. NO induces mitochondrial biogenesis in cultured mouse brown adipocytes through PGC-1α expression. Brown adipocytes were cultured for 4 days with or without SNAP (100 μM), oxyhemoglobin (50 μM, Hb), ODQ (1 μM), 8 Br-cGMP (1 mM), PGC-1α antisense morpholino oligonucleotide (1.7 μM, AS), or control morpholino oligonucleotide with four mis-pairs (1.7 μM, Co) as indicated. The following parameters were then evaluated: (**A**) and (E, inset) mtDNA [one experiment representative of five gels; the numbers in (A), (C), and the inset to (E) show the relative values from the densitometric analysis when control measurements are given a value of 1.0; M, DNA marker; C, controls)]. (**B**) MitoTracker Green fluorescence (expressed as mean relative fluorescence intensity ± SEM over unstained cells; $n =$ 4 experiments); ***, $P < 0.001$ compared with untreated cells; †††, $P < 0.001$ compared with cells treated with SNAP alone. (**C**) Mitochondrial COX IV and Cyt c proteins, detected by immunoblot analysis (one experiment representative of five reproducible ones). (**D**) Transmission electron microscopy (magnification × 22,250; M and N refer to mitochondria and nucleus, respectively). (**E**) PGC-1α, NRF-1, and mtTFA mRNA, analyzed by means of quantitative reverse transcriptase–polymerase chain reaction analysis with gene-specific oligonucleotide probes. Specific fluorescence was monitored during the complete amplification process, compared with glyceraldehyde-3-phosphate dehydrogenase fluorescence as an internal control, and expressed as arbitrary units versus values obtained in untreated cells taken as 1.0 ($n = 5$ experiments). *, $P < 0.05$ compared with untreated cells; †, $P < 0.01$ compared with cells treated with SNAP alone.

Downloaded from www.sciencemag.org on March 2, 2007

tion pathway(s). NO inhibits mitochondrial respiration through direct (cGMP-independent) binding to Cyt c oxidase (*13*). The cGMP dependency of NO-induced mitochondrial biogenesis suggests that it is not due to a mitochondrial response to inhibition of respiratory function.

We next investigated whether NO-induced mitochondrial biogenesis may also occur independently of differentiation processes and in cell types unrelated to brown adipocytes. The effects of NO were studied in mouse white fat 3T3-L1 cells (*14*), which do not undergo differentiation when treated with NO donors as assessed by morphology, lipid droplet (red oil) staining, gene expression, and lipolysis. Effects were also studied in the human monocytic U937 cell line. Results were similar to those observed with brown adipocytes (figs. S1 and S3). Stimulation of mitochondrial biogenesis by NO through cGMP is therefore not restricted to brown adipocytes and their differentiation processes.

In our experimental conditions, brown adipocytes and 3T3-L1 cells expressed only endothelial NO synthase (eNOS) (fig. S4), whereas U937 cells did not express any NOS isoform (*15*). To investigate the role of endogenous NO, we used HeLa cells stably transfected with eNOS under a doxycycline-responsive promoter (*5*, *16*). These cells do not express any other NOS isoform (*16*). eNOS, induced in HeLa cells removal of doxycycline for 72 hours (dox– cells), retained the characteristics of the native enzyme in terms of intracellular localization, functional activity, and level of expression (*16*). eNOS induction significantly increased mtDNA content (by 42 ± 3.1%, $P < 0.01$ versus dox+ control cells, $n = 5$ experiments) (Fig. 2A), COX IV and Cyt c protein levels (by 112 ± 21% and 142 ± 11%, respectively; $P < 0.01$, $n = 5$ experiments) (Fig. 2B), the MitoTracker fluorescence signal (Fig. 2C), and PGC-1α gene expression (Fig. 2D). NRF-1 and mtTFA mRNA levels were only slightly increased. These actions were abolished by the NOS inhibitor L-NAME, which had no appreciable effect in dox+ cells (Fig. 2, A to C). Treatment of the parental HeLa clone with L-NAME had no effect on any parameter measured.

We next studied BAT functions in wild-type and eNOS$^{-/-}$ mice before and after exposure to cold (4°C) for 3 days. Macroscopic examination showed that the interscapular BAT of male and female eNOS$^{-/-}$ mice, acclimatized to either room temperature or low temperature, was a pale-brownish tissue with poorly defined boundaries and mixed with white fat. Gross inspection revealed no marked increases in white fat depots of eNOS$^{-/-}$ mice compared to wild-type mice. Histological sections of BAT from eNOS$^{-/-}$ mice showed a number of adipocytes filled with large lipid droplets and a marked decrease in multilocular adipocytes, a feature typical of functionally inactive tissue (*17*) (Fig. 2E). Accordingly, both BAT UCP1 and PPARγ (the nuclear receptor involved in adipogenesis) mRNA levels were lower in

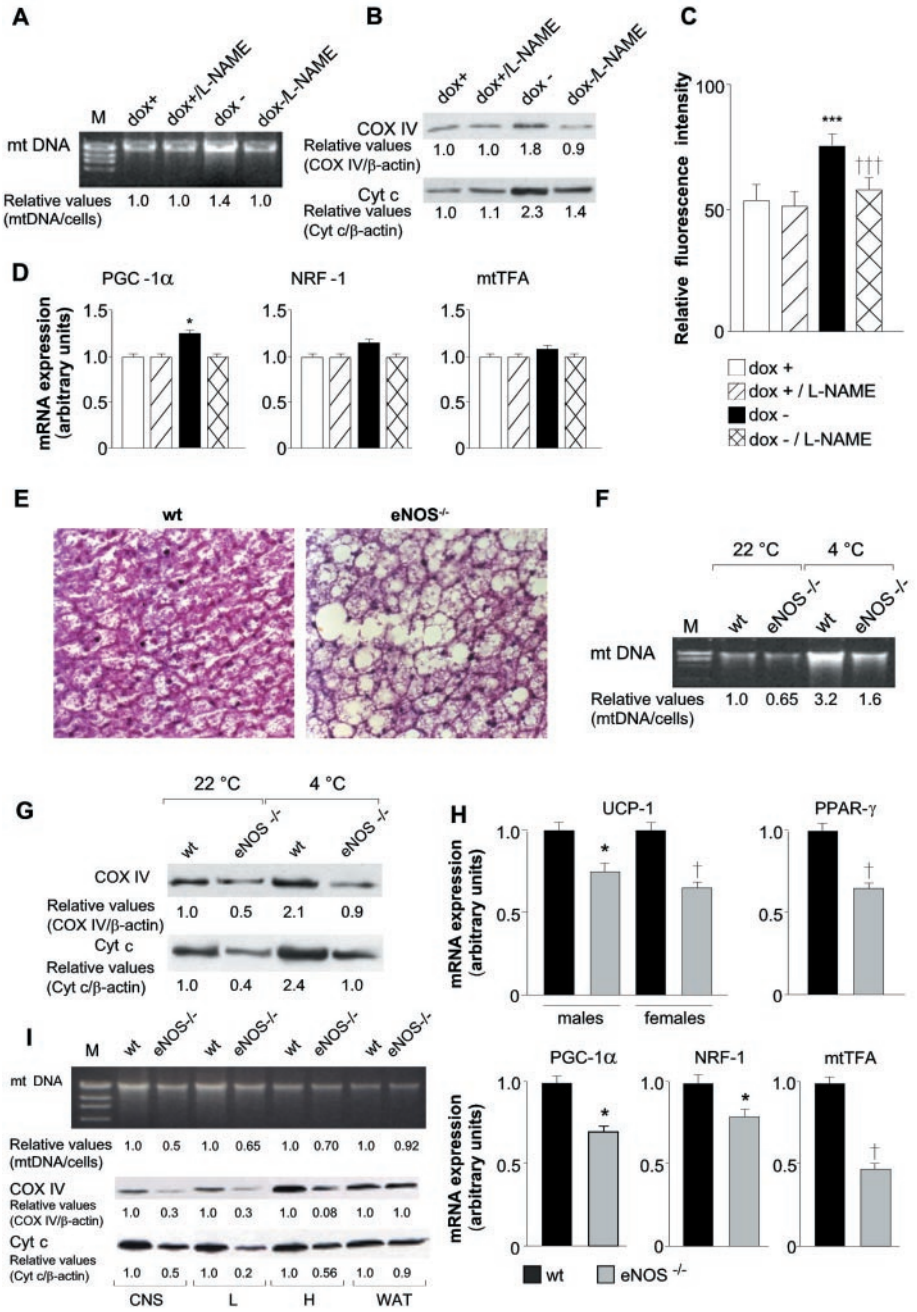

Fig. 2. eNOS expression and mitochondrial biogenesis. (**A** to **D**) Expression of eNOS in HeLa cells (dox–) induces mitochondrial biogenesis with respect to control eNOS-devoid cells (dox+) and eNOS-expressing cells treated with the NOS inhibitor L-NAME (dox–/L-NAME), measured as (A) mtDNA content, (B) COX IV and Cyt c protein levels, (C) MitoTracker Green fluorescence, and (D) PGC-1α, NRF-1, and mtTFA mRNA levels. Each experiment was repeated at least three times. *, $P < 0.05$ compared with control cells; ***, $P < 0.001$ compared with control cells, †††, $P < 0.001$ compared with untreated dox– cells. (**E** to **H**) Reduced mitochondrial biogenesis in female eNOS$^{-/-}$ mice compared with wild-type (wt) mice, as shown by (E) hematoxylin-eosin–stained BAT sections (magnification ×400), (F) mtDNA content, (G) COX IV and Cyt c protein levels, and (H) expression of PGC-1α, NRF-1, and mtTFA genes. (E) and (H) show results in wild-type or eNOS$^{-/-}$ mice exposed to cold for 3 days. *, $P < 0.05$, and †, $P < 0.01$, compared with wild-type mice ($n = 3$ experiments). (**I**) mtDNA content and COX IV and Cyt c protein levels in different tissues from eNOS$^{-/-}$ and wild-type mice. CNS, brain; L, liver; H, heart; M, DNA marker; WAT, white fat. Panels (A), (B), (E), (F), (G), and (I) show one experiment that is representative of three reproducible ones. See the Fig. 1 legend for methodological details.

Downloaded from www.sciencemag.org on March 2, 2007

eNOS$^{-/-}$ mice (Fig. 2H). Furthermore, mtDNA content and COX IV and Cyt c protein levels were lower in female eNOS$^{-/-}$ mice than in female wild-type mice both at room temperature and low temperature (Fig. 2, F and G). This was also true for PGC-1α, NRF-1, and mtTFA mRNA levels (Fig. 2H). This control of mitochondrial biogenesis under basal conditions was not evident when brown adipocytes were cultured in vitro (Fig. 1). This might be because eNOS-activating stimuli that occur in vivo (*3*) may not be present in vitro.

We then investigated NO-induced control of mitochondrial biogenesis in different tissues from wild-type and eNOS$^{-/-}$ animals. Brain, liver, and heart tissue from eNOS$^{-/-}$ mice showed reduced levels of mtDNA, COX IV, and Cyt c as compared with wild-type controls (Fig. 2I). This was not observed in white fat tissue, which contains few mitochondria (*17*). Thus, although these other tissues expressed neuronal and possibly inducible NOS under basal conditions, eNOS deletion was sufficient to reduce mitochondria.

Although the rectal temperature, locomotor activity, and fine movements of eNOS$^{-/-}$ mice were normal (fig. S5, A to D), oxygen consumption rates (*5*) normalized to body mass, a proxy for metabolic rate, were decreased in the fed state at room temperature (24.5° to 25.5°C) by 16 ± 1% and 20 ± 2% ($P < 0.01$ versus wild-type mice, $n = 6$ or 7 experiments) in male and female eNOS$^{-/-}$ mice, respectively (Fig. 3A). The respiration value was not basal because it was measured in pre–cold-stressed animals, i.e., at room temperature. Thus, eNOS deficiency is associated with reduced energy expenditure, suggesting an impairment of BAT-dependent thermogenesis.

Because defective energy expenditure is involved in increased food intake and body weight gain in genetic models of obesity (*18*), we investigated the effects of eNOS deletion on these parameters. Eight-week-old eNOS$^{-/-}$ mice, acclimatized to social isolation for 7 days, were maintained at room temperature (24.5° to 25.5°C) on a regular chow diet, and food intake was measured for 14 days. No appreciable difference was observed in either female or male eNOS$^{-/-}$ mice (Fig. 3B) (mean consumed food per 100 g of body weight per day was 24.7 ± 0.21 g in female –/– mice versus 24.3 ± 0.27 g in female +/+ mice and 19.7 ± 0.31 g in male –/– mice versus 18.37 ± 0.82 g in male +/+ mice, $n = 10$ male and 10 female mice). Despite this, both male and female eNOS$^{-/-}$ mice displayed greater feed efficiency (weight gain per food intake) than their wild-type counterparts (Fig. 3C). Furthermore, at 8 weeks, female and male eNOS$^{-/-}$ mice weighed 24 and 18% more than controls, respectively. These differences were still present at 12 months (Fig. 3, D and E). Thus, increased feed efficiency due to defective energy expenditure could account for the increased body weight in eNOS$^{-/-}$ mice.

Our results show that NO generated by eNOS plays a role in mitochondrial biogenesis in a cGMP-dependent manner. eNOS-deficient animals exhibit reduced mitochondrial number, reduced energy expenditure, weight gain, insulin resistance (*19*), and hypertension (*20*), which are typical features of the metabolic syndrome (*21*). If our results are applicable to humans, they will provide clues for the prevention or treatment of this condition.

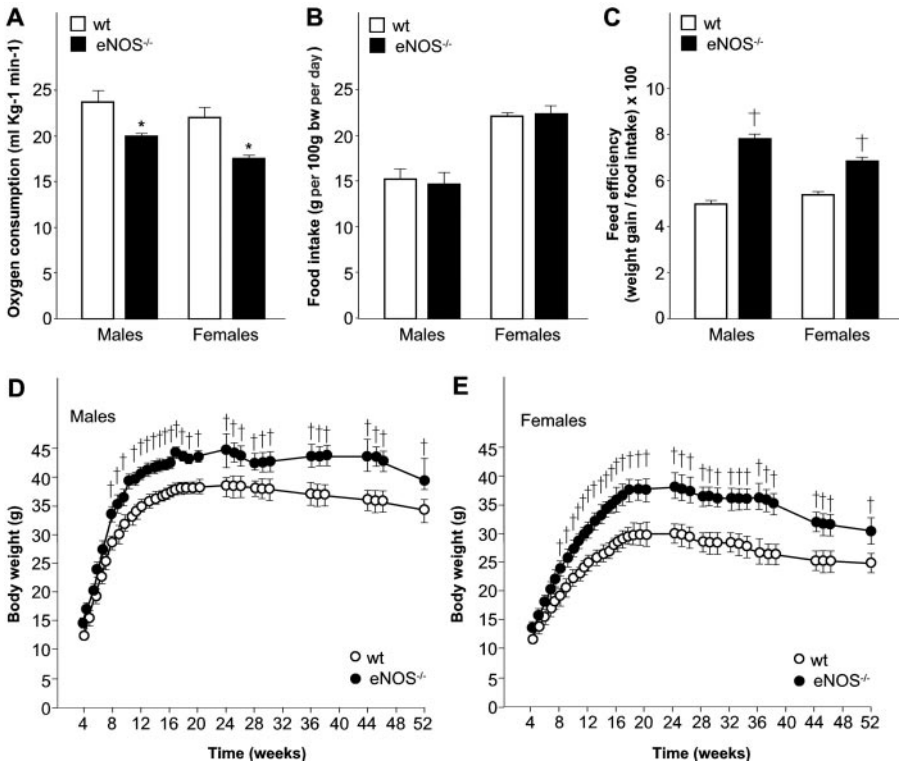

Fig. 3. Oxygen consumption, food intake, feed efficiency, and growth curves of wild-type and eNOS$^{-/-}$ mice. (**A**) Mean oxygen consumption ± SEM from six trials with four wild type and seven trials with four eNOS$^{-/-}$ mice. (**B**) Food intake by 8-week-old wild-type and eNOS$^{-/-}$ mice. Mice were housed individually 7 to 10 days before the experiment and values (mean intake per 100 g of body weight per day ± SEM) were measured for 10 days. (**C**) Feed efficiency, calculated as biweekly weight gain divided by the corresponding food intake, in wild-type and eNOS$^{-/-}$ mice. (**D** and **E**) Body weight of wild-type and eNOS$^{-/-}$ mice housed individually. [(B) to (E)] Male: Wild-type, $n = 8$ mice; eNOS$^{-/-}$, $n = 10$ mice. Female: Wild type, $n = 10$ mice; eNOS$^{-/-}$, $n = 12$ mice; *, $P < 0.05$; †, $P < 0.01$ compared with wild-type mice.

References and Notes

1. D. G. Nicholls, *Biochem. Soc. Trans.* **29**, 751 (2001).
2. E. Nisoli *et al.*, *Br. J. Pharmacol.* **125**, 888 (1998).
3. A. Giordano *et al.*, *FEBS Lett.* **514**, 135 (2002).
4. M. Néchad *et al.*, *Exp. Cell Res.* **149**, 119 (1983).
5. Materials and methods are available as supporting material on *Science* Online.
6. Z. Wu *et al.*, *Cell* **98**, 115 (1999).
7. P. Puigserver *et al.*, *Cell* **92**, 829 (1998).
8. J. J. Lehman *et al.*, *J. Clin. Invest.* **106**, 847 (2000).
9. J. V. Virbasius, R. C. Scarpulla, *Proc. Natl. Acad. Sci. U.S.A.* **91**, 1309 (1994).
10. O. Boss *et al.*, *Biochem. Biophys. Res. Commun.* **261**, 870 (1999).
11. H. Wu *et al.*, *Science* **296**, 349 (2002).
12. J. Lin *et al.*, *J. Biol. Chem.* **277**, 1645 (2002).
13. M. W. Cleeter, J. M. Cooper, V. M. Darley-Usmar, S. Moncada, A. H. Schapira, *FEBS Lett.* **345**, 50 (1994).
14. H. Green, O. Kehinde, *Cell* **5**, 19 (1975).
15. C. De Nadai *et al.*, *Proc. Natl. Acad. Sci. U.S.A.* **97**, 5480 (2000).
16. S. Bulotta, R. Barsacchi, D. Rotiroti, N. Borgese, E. Clementi, *J. Biol. Chem.* **276**, 6529 (2001).
17. S. Cinti, *Proc. Nutr. Soc.* **60**, 319 (2001).
18. J. Himms-Hagen, *Proc. Soc. Exp. Biol. Med.* **208**, 159 (1995).
19. R. R. Shankar, Y. Wu, H. Q. Shen, J. S. Zhu, A. D. Baron, *Diabetes* **49**, 684 (2000).
20. P. L. Huang *et al.*, *Nature* **377**, 239 (1995).
21. E. S. Ford, W. H. Giles, W. H. Dietz, *JAMA* **287**, 356 (2002).

22. We thank A. Higgs for her help with preparation of the manuscript; L. Vizzotto for assistance with light microscopy; F. Gennari for help with figure preparation; R. Scurati for help with food intake and body weight measurements; and E. Ferrannini, J. Meldolesi, and P. Mantegazza for critical support and revision of the manuscript. Supported by grants from the Ministero dell'Istruzione, dell'Università e della Ricerca cofinanziamento 2001 to E.N. and E.C., the Italian Association for Cancer Research to E.C., the Medical Research Council to S.M., and the University of Milan and the Italian Ministry of Health to M.O.C. and E.N.

Supporting Online Material

www.sciencemag.org/cgi/content/full/299/5608/896/DC1
Materials and Methods
Figs. S1 to S5
References and Notes

15 October 2002; accepted 13 December 2002

Downloaded from www.sciencemag.org on March 2, 2007